Modeling and Validation of Flow-Structure Interactions in Passive Micro Valves

R.E. Oosterbroek*, S. Schlautmann, J.W. Berenschot, T.S.J Lammerink,
A. van den Berg and M.C. Elwenspoek

* MESA Research Institute, University of Twente, Faculty of Electrical Engineering,
P.O. Box 217, 7500 AE Enschede, The Netherlands, R.E.Oosterbroek@el.utwente.nl

ABSTRACT

This paper reports the modeling of the stationary flow-structure interaction of different types of micro check valves. Mathematical indirect, domain coupled and de-coupled, finite element models as well as analytical approximations are made. The obtained simulation results are validated by performed measurements on fabricated micro valves. Simple analytical formulas are derived. These can be used for micro fluid handing component design purposes as well as for input for numerical lumped element system simulation programs.

Keywords: valves, CFD, FEM, domain coupling, μ-TAS

INTRODUCTION

In the field of chemical analysis, there is need for small, portable and cheap (disposable) systems of chemical and physical sensors and actuators. With use of micro mechanical fabrication techniques we aim at fabricating such components and integrating them into a so called "Micro Total Analysis System" (μ-TAS) [1]. These miniaturized systems benefit from the possibility of fast chemical, mechanical and fluid dynamical responses due to small internal volumes. To predict the stationary as well as dynamical responses of the micro fluid handling components, such as valves, we need design tools. For dynamic system modeling with bond-graph methods, like 20-SIM [2], flow and effort transfer between lumped elements must be described. These programs require input of the component behavior in the form of (simple) analytical formulas. For elementary structures like circular tubes, analytical formulas can be derived without any problem. For more complex geometries, numerical tools are needed, based on discretization principles like finite elements (FEM) [3].

PASSIVE MICRO VALVES

In fluid handling systems, micro check valves play an important role. With use of the diode function, fluid streams can be directed. This type of valve provides the possibility to build micro pumps like it is demonstrated by Van Lintel et. al. [4]. A direction dependent pressure drop over the valve is obtained due to flow-pattern related changes, such as with the diffuser-nozzle principle [5], or due to reduction of the cross-area when the flow is reversed. In this paper, the four types of valves, listed in figure 1. are discussed. The pressure drop / flow-rate relations are researched numerically and analytical approximations are made.

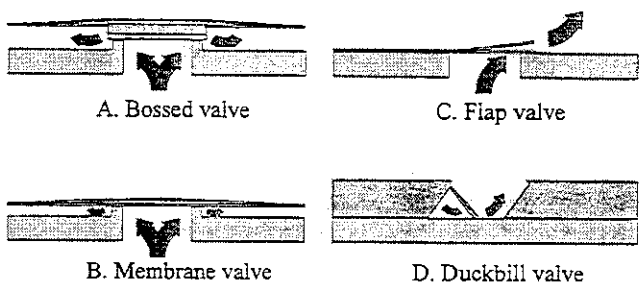

Figure 1. Modeled passive check valve types

Valve A. consists of a rigid boss which is suspended by four flexible beams. If a flow-stream is applied, coming from the bottom, the pressure drop over the valve will result in a lift of the boss. An opposite pressure drop will press the boss against the valve seat and closes the valve.

A membrane valve only consists of a flexible membrane. Besides a lift of the membrane, also a deformation of the flow-area arises, depending on the applied flow rate.

The flap valve consists of a flexible plate, clamped at one side. If flow is applied at the bottom, the plate will bend up and the fluid flows through. In the opposite direction, the plate will be pushed against the substrate which closes the gap.

Finally, the duckbill valve (D) is shown, which is functioning according to the same principle [7]. However, the plate is now positioned under the crystallographic angle of 54.7 degrees as a result of an-isotropic KOH etching of a [100] wafer. Besides this, the plate is fully clamped at three edges instead of one, which results in a curved, sinusoidal flow-opening.

ANALYTICAL MODELING

Introduction

For modeling the pressure drop over the valve and the lift height as a function of the flow-rate, we have to deal with the coupling between the solid mechanical and fluid mechanical domains. The pressure drop over the valve can be computed from the flow-profile of the fluid. However, the flow-profile is related to the pressure-induced (elastic) geometry deformation of the valve. Mathematically written:

$$\Delta P = R(\Delta P) \cdot \Phi$$

Where ΔP and Φ are the pressure and volume flow-rate respectively and R the pressure sensitive valve resistance. This mathematical domain-coupled problem can be solved in three ways:

1. The non-linear partial differential equations for the mechanical structure and the fluid can be (iteratively) numerically solved in one matrix system.
2. The differential equations for both domains can be solved separately, after which the computed pressure or deformation data is transferred. By substitution of the computed data of one domain into the equations of the second domain and vice versa, an iteration procedure is obtained towards an equilibrium situation (mathematical in-direct coupled solving).
3. The physical domain coupling degrees of freedom can be reduced to one. Both domains can be computed separately after which the computed data can be linked. This, we called mathematical domain de-coupling.

Bossed valve

The third method is very suitable for obtaining analytical approximations. However, it is only usable if reduction to one degree of freedom is valid. For the bossed valve this is possible under the following two assumptions:

- The boss is has a high stiffness compared to the springs
- The boss will only lift vertically, without tilting

With this, all displacements are reduced to only the lift of the boss. A relation between the force, acting on the boss due to a pressure drop, can be set-up as well as a pressure-flow rate relation as function of this gap. Both equations can be linked together by the lift parameter.

For a circular boss, suspended by four beams, with dimensions as shown in figure 2, we found the relation:

$$Eu^4 \cdot Re_r = \frac{96}{\pi^4} \cdot \Pi_{stiff}^{\ 3} \cdot \frac{\left(\ln \Pi_{geom}\right)^4}{\left(\Pi_{geom}^{\ 2} - 1\right)^3}$$

Where:

$Eu = \frac{\Delta p \cdot r_{inlet}^{\ 4}}{\frac{1}{2} \cdot \rho \cdot \Phi^2}$, the Euler number

$Re_r = \frac{\rho \cdot \Phi}{\mu \cdot r_{inlet}}$, the Reynolds number

$\Pi_{stiff} = \frac{k_m \cdot r_{inlet}^{\ 3}}{\frac{1}{2} \cdot \rho \cdot \Phi^2}$, the dimension-less stiffness

$\Pi_{geom} = \frac{r_{outlet}}{r_{inlet}}$, the in-/outlet aspect ratio

with ρ the mass density (kg/m^3), μ the dynamic viscosity (kg/ms) and k_m the spring constant (N/m).

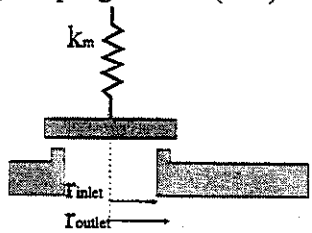

Figure 2: The used parameters for the bossed valve.

In this relation we assumed the valve seat to be relatively wide, such that the entrance and exit effects are neglected and a parabolic Poiseuille flow-profile [8,9] is present over the full length of the gap.

Membrane valve

For the membrane valve, the assumption can be made that for small deflections, the membrane still is positioned parallel to the seat. This results in the following equations for the resistance:

$$Eu_r^{\ 4} \cdot Re = 1.00 * 10^6 \cdot \frac{\Pi_{stiff}^{\ 3}}{\Pi_{geom1}^{\ 6}} \cdot \frac{\ln\left(\Pi_{geom2}\right)}{\left(1 + \Pi_{geom2}\right)^6}$$

With Eu, Re the Euler and Reynolds numbers respectively, similar to the bossed valve.

$\Pi_{stiff} = \frac{D \cdot r_{inlet}}{\frac{1}{2} \cdot \rho \cdot \Phi^2}$ the dimension-less stiffness

$\Pi_{geom1} = \frac{r_{membrane}}{r_{inlet}}$ the dimension-less membrane size

$\Pi_{geom2} = \frac{r_{outlet}}{r_{inlet}}$ the dimension-less seat size

$D = \frac{Eh^3}{12(1-\nu^2)}$ the bending stiffness of the membrane

Under the restriction: $\Pi_{geom1} >> \Pi_{geom2}$, so for a large membrane radius $r_{membrane}$ and a small valve seat.

Flap valve

The flap valve was modeled by assuming that the angle of the bent, 2D modeled plate is constant at the valve seat. Because side effects are not taken into account, the model will resemble reality better for wide plates. The dimensionless formula, describing this valve is:

$$Eu^4 \cdot Re = 4.92 * 10^4 \cdot \frac{\Pi_{stiff}{}^3}{\Pi_{geom1} \cdot (\Pi_{geom2} + 1)^9} \cdot \left[\frac{1}{(7 - \Pi_{geom2})^2} - \frac{1}{(7 \cdot \Pi_{geom2} - 1)^2} \right]$$

$$Eu = \frac{\Delta p \cdot a^4}{\frac{1}{2} \cdot \rho \cdot \Phi^2} \qquad Re_a = \frac{\rho \cdot \Phi}{\mu \cdot a}$$

$$\Pi_{stiff} = \frac{h^3 \cdot E \cdot a}{\frac{1}{2} \cdot \rho \cdot \Phi^2} \qquad \Pi_{geom2} = \frac{1}{a}$$

$$\Pi_{geom1} = \frac{w}{a} \qquad \text{for } \Pi_{geom2} < 7$$

Where w the in-plane oriented width of the flap.

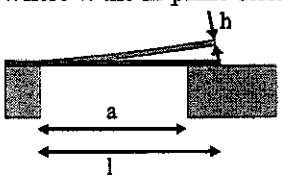

Figure 3: Used parameters in describing the flap valve characteristic

Duckbill valve

Due to the three sided clamping, the plate of the duckbill valve shows a curved shape. A series approximation is given by W.J. van der Eb [10]. However, we used a more simple series approximation given by Timoshenko [11], for a one sided clamped and two sided simply supported plate:

$$w = \frac{4 Q a^4}{\pi^5 D} \sum_{m=1,3,5..}^{\infty} \frac{1}{m^5} (1 - \hat{Y}_m) \sin(x_m)$$

$$\hat{Y}_m = (1 + C_m y_m) \cosh y_m - (B_m y_m + C_m) \sinh y_m$$

$$x_m = \frac{m\pi x}{a} \qquad y_m = \frac{m\pi y}{a}$$

$$B_m = \frac{(3+\nu)(1-\nu)\cosh^2\beta_m + 2\nu\cosh\beta_m - \nu(1-\nu)\beta_m \sinh\beta_m - (1-\nu^2)}{(3+\nu)(1-\nu)\cosh^2\beta_m + (1-\nu)^2\beta_m^2 + (1+\nu)^2}$$

$$C_m = \frac{(3+\nu)(1-\nu)\sinh\beta_m \cosh\beta_m + \nu(1+\nu)\sinh\beta_m - \nu(1-\nu)\beta_m \cosh\beta_m - (1-\nu)^2\beta_m}{(3+\nu)(1-\nu)\cosh^2\beta_m + (1-\nu)^2\beta_m^2 + (1+\nu)^2}$$

$$\beta_m = \frac{m\pi b}{a}$$

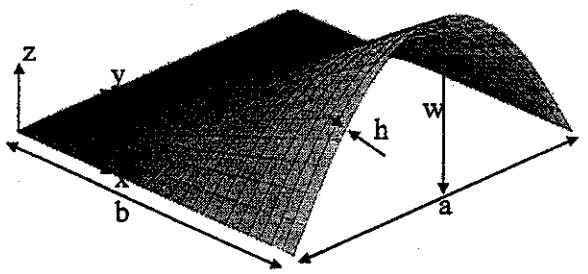

Figure 4: Computed deformation shape of the membrane and the used geometric parameters

The gap size for the throughput of the flow is computed by multiplying this result with the cosine of 54.7 degrees due to the crystallographic orientation: w_P=w(b).cos(54.7). Assuming a fully developed Poiseuille flow, the resistance of the valve is computed with:

$$R(\Delta P) = \frac{12\mu h}{\int_{y=0}^{a} w_P(y)^3 dy}$$

This integral has been evaluated numerically. Results of the flow-rate and change of width, a, of the valve are plotted in a three-dimensional plot in figure 4.

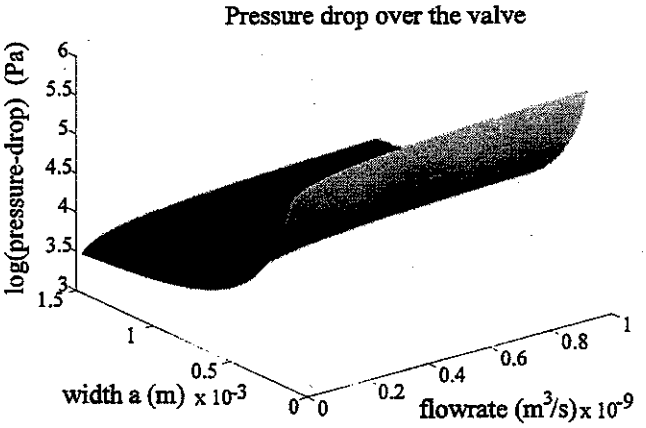

Figure 5: Pressure drop over a 5μm thick and 300μm high valve as function of the flow-rate and width.

NUMERICAL MODELING

Introduction

To verify the analytical models and to improve these approximations, numerical computations are performed. With the numerical simulations we can model more complex geometric structures and take neglected effects into account such as entrance and exit effects and mechanical non-linearities for large deflections. These numerical computations were performed with the ANSYS 5.3 / Flotran package, running on a Pentium 120 - Windows NT platform. Code is programmed in this package, using the APDL language [12]. For the bossed and the duckbill

valve, the method of de-coupling was used to save computation time. The other valves were computed using the mathematical indirect coupled method of iterative data substitution between the fluid dynamical and solid mechanical FEM simulations.

Domain de-coupling

De-coupling of the two domains is done by regarding only one degree of freedom in the mechanical domain (deflection). Therefore we only need to build a loop in which for a range of different lift heights and valve seat dimensions, the pressure drop over the valve is computed at a certain flow-rate. This pressure drop can be integrated over the boss or membrane to find the force, acting on it. If we know the spring-constant of the valve or the load-deflection curve, an equilibrium point is found where the force, generated by the spring, balances the integrated pressure drop. For linear mechanical behavior, the spring constant of the valve can easily be computed analytically because only one degree of freedom is taken into account.

Because values need to be filled-in when performing FEM computations, we would need to perform a lot of runs to cover all possible configurations of lift heights, valve dimensions and material properties. Therefore the dimension-less parameters, similar to those, introduced for the analytical models, are used to reduce the number of independent parameters to a minimum set.

Domain coupled solving

During the coupled-solving process, both domains are computed separately. The pressure profile, computed by the CFD (computational fluid dynamics) module must be transferred to generate the load on the solid structure. In the solid mechanics module, the induced deformation is computed. After this, the geometry of the mathematical grid, used in the CFD module, needs to be updated and so on. This process continues until a certain convergence level is obtained, defined in terms of deformation. Our implementation is shown in the flow-diagram in figure 6. The basic ideas behind this implementation are flexibility in:

- Geometry and boundary condition definitions.
- Definition of the convergence criterion.
- Definition of the load and deformation transfer.
- Numerical grid optimization.

Implementing types of valves, with different geometries and sizes is facilitated by using a parametric description in combination with "components". With these elements, new objects can be defined which refer to a selection of areas, lines or grid nodes. Boundary descriptions such as fixed wall, entrance and exit conditions, are defined on these objects.

For different situations we may want to use a different convergence criteria. For valves, the convergence criterion will usually be the normed relative deformation change between two subsequent iteration steps n and n-1:

$$\varepsilon_n \leq \frac{\|h_n - h_{n-1}\|}{\|h_n\|}$$

The number of grid points, h, to take into account may change. When computing a clamped membrane, only the center point, but also the whole membrane surface can be taken into account. Therefore we used "component" objects to be flexible in defining the convergence criterion.

During the equilibrium iterations, the nodal pressure solutions of the CFD simulation must be transferred to the mechanical structure. One possible way to do this is a definition of a list of interface node numbers of the CFD computation with their corresponding counterparts in the structural domain [13].

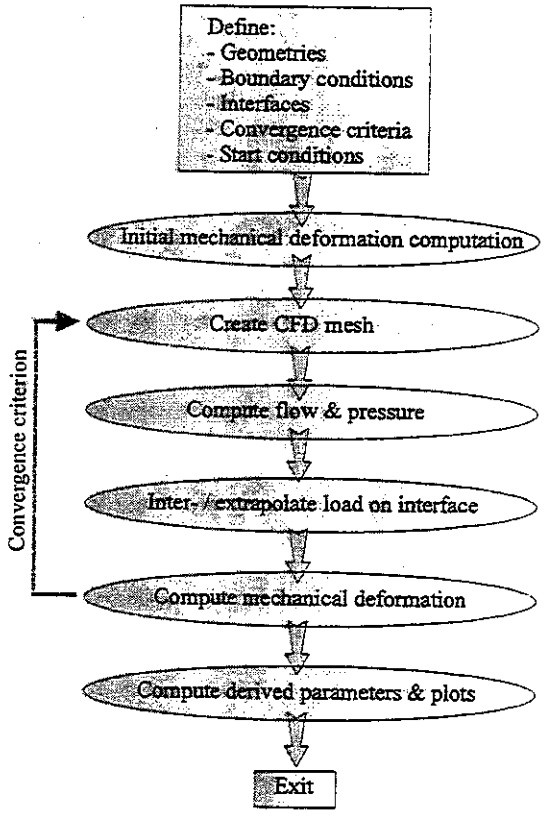

Figure 6: Flow diagram of the domain coupled FEM code.

In our implementation, this procedure is automated by assigning interface components. A one to one connection of nodal interface values in different domains would create a numerically inflexible program. Usually, convergence during fluid dynamical computations is much more difficult to obtain than of solid mechanics. Mesh refinements are needed where large pressure and velocity gradients are expected. For structural computations however, these induced local loads have little effect on the total

deformation profile. Local stress peaks, quickly vanish at some distance according to Saint-Venant's principle [14]. This means that the numerical grids for the CFD and structural computations are optimized, using different grid sizes on the interface.

The restriction of using identical numerical grids at the interfaces due to domain coupling hampers individual grid optimization. This drawback can be overcome by interpolation of the interface data. With this method it also becomes possible to use elements of different order (e.g. quadratic fluid elements and bi-linear structural elements) and to reduce the needed amount of elements. If wished, the number of elements and the grids can even be varied during the iterative solving process.

RESULTS

In figure 7 the flow field in the flap valve is shown (unity scaled). This is one specific simulation out of a range of coupled simulations which were needed to cover the design space of this valve. During the iterations, the geometry is constantly updated. For the first steps, when there is a big difference with the equilibrium situation, these updates can be big from step to step. During these geometry changes, the numerical grid must be updated as well. This might lead to the possibility of divergence because the number of elements of the grid is not changed. A solution for this problem is to start with conditions, near to the wanted equilibrium. This problem is also met when, in the loop over the geometric parameter changes, the elements turn to become poorly shaped. It means that the parameter range in the loop is limited by the possibility on convergence with the used numerical grid. To overcome the problem of divergence, a more smart grid mesh processor is needed. We related the number of elements to the specific lengths which define the mesh area.

From the simulation results, the pressure drop was computed and fitted on the formulas which were obtained by using the dimension-less parameters. For each valve, the following relations were found:

For the bossed valve:

$$Eu^4 \cdot Re = \frac{16}{\pi^3} \cdot C_1 \cdot \Pi_{stiff}{}^3 \cdot \frac{\left(\ln \Pi_{geom}\right)^3}{\left(\Pi_{geom}{}^2 - 1\right)^3} \cdot \left[\left(\ln \Pi_{geom}\right) + C_2\right]$$

with C_1=1.91 and C_2=3.97*10^{-2}

The fitted value C_1 equals the analytical approximation. This function, rewritten in dimensional form, for a specific situation, together with the analytical as well as the measured results is plotted in figure 9. The pressure-fow rate relation for the other type of valves show the same strongly non-linear shape.

For the membrane valve we found:

$$Eu_r{}^4 \cdot Re = 1.36 * 10^6 \cdot \frac{\Pi_{stiff}{}^3}{\Pi_{geom1}{}^6} \cdot \frac{\ln\left(\Pi_{geom2}\right)}{\left(1 + \Pi_{geom2}\right)^6}$$

For the flap valve:

$$Eu^4 \cdot Re_a = C \cdot \frac{\Pi_{stiff}{}^3}{\Pi_{geom1} \cdot \Pi_{Geom2}} \qquad C=6.86*10^{-1}$$

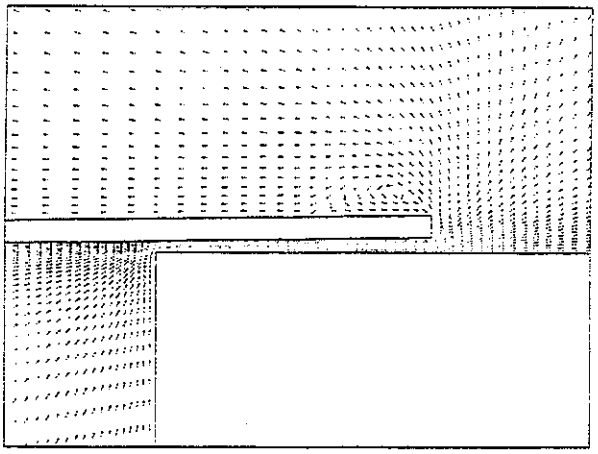

Figure 7: Flow-field of a silicon flap-valve with dimensions: thickness 8µm, length 500µm, width 100µm at a flow rate of 0.04µl/s, computed with the indirect numerically coupled FEM method.

And for the duckbill valve for small deflections:

$$Re \cdot Eu^4 = \frac{9 \cdot \pi^{16} \cdot \Pi_{stiff}{}^3}{32 \cdot \Pi_{geom1}{}^{13} \cdot \Pi_{geom2}{}^3} + \frac{34.11 \cdot \pi^{10} \cdot \Pi_{stiff}{}^2 \cdot Eu}{8 \cdot \Pi_{geom1}{}^9 \cdot \Pi_{geom2}{}^2}$$

$$Re = \frac{\rho \cdot \Phi}{\mu \cdot t}, Eu = \frac{p \cdot h^4}{\frac{1}{2} \cdot \rho \cdot \Phi^2}, \Pi_{stiff} = \frac{D \cdot t}{\frac{1}{2} \cdot \rho \cdot \Phi^2}, \Pi_{geom1} = \frac{a}{t}$$

$$\Pi_{geom2} = \sum_{m=1,3,5\ldots}^{\infty} \frac{\left(1 - \hat{Y}_m\right)}{m^5} \cdot \sin\left(x_m\right) \cdot \cos(54.7°) \Big|_{x=\frac{a}{2}, y=b}$$

where $\hat{Y}_m$ equals the shape function, found for the analytical approximation of the three-sided clamped plate.

MEASUREMENTS

To validate the derived formulas for the bossed valve, micro valves where made and characterized. Although the boss originally was designed to be square due to the restrictions of the bulk micromachining process (KOH etching) , we modeled it axi-symmetric. Despite of the geometric simplification, this simplified finite element model still shows a good correspondence with the measurements as is shown in figure 8. The analytical model shows less resistance, especially at higher flow-rates. This difference is due to the neglect of the entrance and exit effects. At low flow rates, the gap of the valve is small so that the neglected

effects do not play a dominant role. At higher flows, the entrance and exit effects become more important and need to be taken into account.

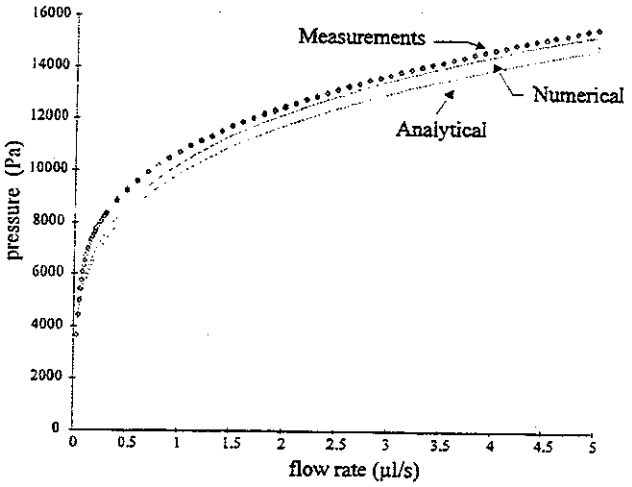

Figure 8: Comparison between the analytical, numerical and measured flow-pressure drop relations

From the formula, describing the pressure-flow relation of the bossed valve, it can be seen that the pressure drop is very sensitive to the beam height of the springs. The beam height is related to the power 3*3/4 = 9/4 to the pressure drop. This high thickness sensitivity of the valve behavior means that an extremely high manufacturing precision is required to process micro check valves, showing specified flow-pressure characteristics.

CONCLUSIONS

To predict the behavior of bossed, membrane, flap and duckbill type of check valves, we built analytical as well as finite element models. The FEM models consist of solving both, fluid and structural domains, iteratively by transfer of load and displacement data as well as de-coupled. All geometry, load descriptions and data transfer are geometry based instead of node based. This allows a great flexibility in building different models. Also other physical domains can be coupled. This coupling is facilitated by the use of inter- / extrapolation of data between the different domains. With this feature, both numerical grids can be optimized to improve convergence. Good grid meshing during these procedures remains a major point of attention.
With the numerical computations, the analytically obtained models are verified and extended by fitting on dimension-less formulas. For the bossed valve, measurements are performed. The analytical and FEM models describe the pressure-flow relation well. However, because the resistance characteristic of the valve is very sensitive to the beam height, high fabrication precision is needed to meet computed behavior.

REFERENCES

1. M.C. Elwenspoek, T.S.J. Lammerink, R. Miyake, J.H.J. Fluitman, "Towards Integrated Microliquid Handling Systems", Journal of Micromechanics and Microengineering (4), pp. 227-245, 1994
2. P.C. Breedveld, "Dynamische Systemen: Modelvorming en Simulatie met Bondgrafen", Open Universiteit ISBN 90-358-1302-2, 1994
3. R.D. Cook, D.S. Malkus, M.E. Plesha, "Concepts and Applications of Finite Element Analysis", JohnWiley & Sons Inc., Third edition, 1989
4. H.T.G. van Lintel, F.C.M van de Pol, S. Bouwstra, "A Piezoelectric Micropump Based on Micro-machining of Silicon", Sensors and Actuators, 15, 1988, pp. 153-167
5. E. Stemme, G. Stemme, "A Valveless Diffuser / Nozzle-Based Fluid Pump", Sensors and Actuators A, 39, 1993, pp. 159-167.
6. P. Gravesen, J. Branebjerg, O. Søndergård Jensen, "Microfluidics - a Review", Micromechanics and Microengineering (3), pp. 168-182, 1993
7. R.E. Oosterbroek, J.W. Berenschot, S. Schlautmann, T.S.J Lammerink, A. van den Berg, M.C. Elwenspoek, "In-plane Oriented Fluid Control Components, Fabricated with New Etching Techniques", Actuator98, Bremen, Germany, 1998
8. R.W. Fox, A.T. McDonald, "Introduction to fluid mechanics", John Wiley & Sons, Third edition, 1985
9. F.W. White, "Fluid mechanics", McGraw-Hill, Third edition, 1994.
10. W.J. Van der Eb, "Berekeningen van een Plaat, welke aan 3 Zijden Ingeklemd en aan de 4e Zijde Geheel Vrij is", De Ingenieur,Vol. 26, June 1950, pp. O.31-O.35
11. S.P. Timoshenko, S. Woinowski-Krieger, "Theory of Plates and Shells", Mc. Graw-Hill Int., Second edition 1970, pp. 211-214
12. G. Müller, I Rehfeld, W. Katheder, "FEM für Praktiker", Expert Verlag, Second edition, 1995
13. J.C.C. van Kuijk, "Numerical modelling of flows in micro mechanical devices", University of Twente, June 5, 1997, ISBN 90-9010395-3
14. S.P. Timoshenko, J.N. Goodier, "Theory of Elasticity", Mc. Graw-Hill Int., Third edition, 1970, pp. 39-40